Available online at www.sciencedirect.com
SCIENCE DIRECT®
Journal of Nuclear Materials 329–333 (2004) 1228–1232
journal of nuclear materials
www.elsevier.com/locate/jnucmat

Dislocation–stacking fault tetrahedron interaction: what can we learn from atomic-scale modelling ☆

Yu.N. Osetsky *, R.E. Stoller, Y. Matsukawa

Oak Ridge National Laboratory, Computer Sciences & Mathematics Division, Bldg. 4500S, MS-6138, P.O. Box 2008, Oak Ridge, TN 37831-6138, USA

Abstract

The high number density of stacking fault tetrahedra (SFTs) observed in irradiated fcc metals suggests that they should contribute to radiation-induced hardening and, therefore, taken into account when estimating mechanical properties changes of irradiated materials. The central issue is describing the individual interaction between a moving dislocation and an SFT, which is characterized by a very fine size scale, ~100 nm. This scale is amenable to both in situ TEM experiments and large-scale atomic modelling. In this paper we present results of an atomistic simulation of dislocation–SFT interactions using molecular dynamics (MD). The results are compared with observations from in situ deformation experiments. It is demonstrated that in some cases the simulations and experimental observations are quite similar, suggesting a reasonable interpretation of experimental observations.

1. Introduction

Stacking fault tetrahedra (SFTs) are common defects induced by different treatments, such as irradiation, ageing after quenching and deformation, in fcc metals [1–3] and they are responsible for strengthening, hardening and plastic instability during deformation. Interaction between dislocations moving through the population of the existing SFTs is in the basis of these effects and therefore it is important to understand their mechanisms. Three different approaches, namely experiment, continuum theory and atomistic modelling, are currently used to study the details of dislocation–SFTs interactions. The in situ experimental techniques, when the specimen subjected to transmission electron microscopy is deformed simultaneously, may reveal many important details of the interaction [4,5]. The disadvantage of in situ experiments is low spatial and time resolution, ~100 nm and one image per 1/30 s. This limits observation of only large defects and low strain rate. Continuum theory describes large SFTs as a set of stair rod dislocations and can be applied with an accuracy limited to the details of the dislocation–dislocation interaction considered at continuum level [6]. Temperature and strain rate effects are far beyond of this approach. And finally, atomic-scale modelling can be formally used to investigate all aspects of dislocation–SFT interactions [7–9]. The main limitation is the total time of the interaction limited by a few nanoseconds. Modern large-scale atomic-level models can obtain valuable information, which in some cases can be compared directly with in situ experiments. Here we report first results of an extended programme of atomic-scale modelling of dislocation dynamics in the environment of high density of small, less then ~6 nm, SFTs. This study is a part of multi-scale materials modelling programme aimed to understand the effect of irradiation to mechanical properties of fusion materials.

1.1. Model

Interactions between a moving edge dislocation and SFT have been studied using the atomistic model

☆ Research sponsored by the Office of Fusion Energy Sciences and Division of Materials Sciences and Engineering, US Department of Energy under contract DE-AC05-00OR22725 with UT-Battelle, LLC.
* Corresponding author. Tel.: +1-865 576 3254; fax: +1-865 241 3650.
E-mail address: osetskiyyn@ornl.gov (Yu.N. Osetsky).

0022-3115/$ - see front matter © 2004 Elsevier B.V. All rights reserved.
doi:10.1016/j.jnucmat.2004.04.257

developed in [10] and applied for statics ($T = 0$ K) and dynamics ($T > 0$ K) conditions. The first approach allows to investigate equilibrium state of a system at a certain strain and the results can be compared directly with the continuum dislocation dynamics and used for parameterisation of interaction mechanisms. The second approach allows to investigate temperature and strain rate effects. The main advantage of the model developed in [10] is that stress–strain dependences and therefore the critical resolved shear stress (CRSS) can be obtained at different conditions. In the present work we have simulated fcc crystal of size $46.0\times35.5\times25.7$ nm along the $[1\,\bar{1}\,0]$, $[1\,1\,\bar{2}]$ and $[1\,1\,1]$ axes respectively and containing about 3.5 million mobile atoms interacting via a many-body potential parameterized for copper in [11].

The edge dislocation with initial Burgers vector $\frac{1}{2}[1\,\bar{1}\,0]$ and $(1\,1\,1)$ glide plane was first introduced and relaxed. During relaxation the dislocation dissociated into two Shockley partials separated with a stacking fault of about 3 nm of width. Staking fault tetrahedra of size from 2.5 to 4.1 nm where then created in the vicinity of the dislocation so that the dislocation glide plane intersects the SFT at different level h, which is the distance between the dislocation glide plane (bottom of the extra half plane) and the SFT base. In static modelling strain was incrementally increased by 10^{-4} per step with the following relaxation of the system to the minimum of potential energy. In dynamic modelling strain rate $(2–5)\times10^{6}$ s^{-1} was applied, which results in dislocation velocity from ~10 to ~20 m/s.

Due to lack of space we present here mainly the results obtained for the case of 4.1 nm SFT containing 136 vacancies.

2. Results

An example of stress–strain curves obtained for the case $h = 0.96$ nm at different temperatures is presented in Fig. 1. One can see that the critical resolved shear stress, which is a maximum stress at each curve, depends strongly on temperature and it drops from ~253 MPa at $T = 0$ to 148 MPa at $T = 10$ K and to ~75 MPa at

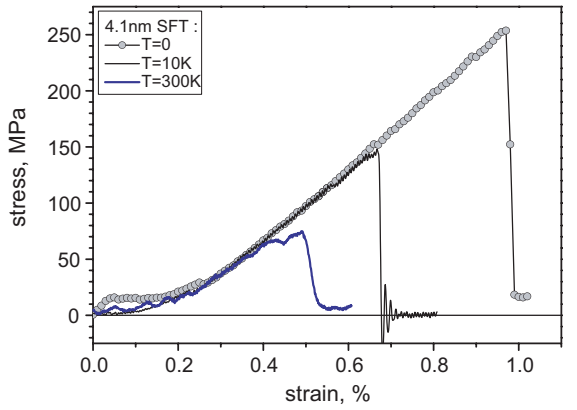

Fig. 1. Applied stress as function of strain in crystal at $T = 0$, 10 and 300 K containing a dislocation gliding through a row of 4.1 nm (136 vacancies) SFT at $h = 0.96$ nm.

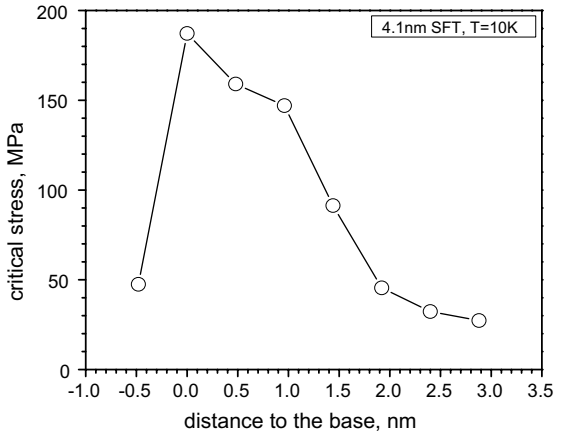

Fig. 2. Dependence of the value of critical resolved shear stress against distance between the dislocation glide plane and the base of a 4.1 nm SFT simulated at $T = 10$ K.

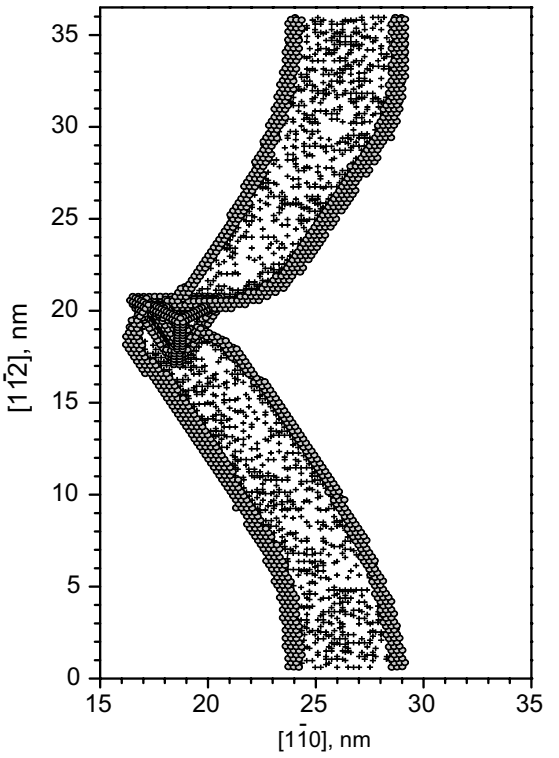

Fig. 3. Dislocation line in the $(1\,1\,1)$ slip plane at the critical stress for 4.1 nm SFT cut at $h = 0.96$ nm at $T = 10$ K. Gray circles are atoms belonging the dislocation core, little crosses are atoms which are definitely in HCP environment.

$T = 300$ K. Note that a significant drop occurs at very low temperature implying that even very small atomic vibrations assist significantly for dislocation to penetrate through the SFT. The stress–strain behaviour depends also on h as it is shown in Fig. 2 for $T = 10$ K where h starts at −0.48 nm (just below the SFT base) and ends at $h = 2.40$ nm (the height of the tetrahedron is equal to ~3.34 nm). The maximum CRSS, 182 MPa, was observed for the case $h = 0$, e.g. when dislocation glide plane coincides with the SFT stacking fault. The overall conclusion is that the CRSS increases as the dislocation glide plane approaches the SFT base inside the SFT volume. The example of the dislocation configuration at critical stress, $\sigma = 148$ MPa, for the case $h = 0.96$ at 10 K is presented in Fig. 3. The shape of the dislocation (circles) and stacking fault area (crosses) can be seen and it is clear that, due to dissociation of the dislocation, the estimation of the critical angle is rather complicated.

The position of the dislocation as it hits the SFT defines also the structural change of the SFT. Thus, if the dislocation hits SFT close enough to its vertex the SFT may not be damaged – the upper part of the SFT is shifted when the leading partial dislocation leaves it but after the trailing partial leaves SFT it recovers its perfect configuration by a collective shift of the corresponding atoms above the glide plane. Such a recovery of the SFT was observed when distance between the glide plane and the vertex is $\leqslant 1.5$ nm. If it is larger the SFT can be damaged in different ways depending on h. Some configurations of the SFT after interaction are presented in Fig. 4. In these figures the size of the cube box is $13a$ ($a = 0.3615$ nm is Cu lattice parameter) and the grid size is $1a$. The damage of the SFT includes formation of two ledges of opposite sign on two faces: I-type ledge is created on the face where the leading partial dislocation entered the SFT and V-type ledge is created on the face where the trailing partial dislocation left it. The detailed configuration of ledges depends on h as it can be seen in Fig. 4(b) and (c). The case $h = 0$, when the whole upper part of the SFT was shifted relatively the stacking fault of the lower base, can be interpreted as a creation of the minimum size ledges (see Fig. 4(d)).

Experimentally observed formation of channels cleared from radiation-induced defects is characterized

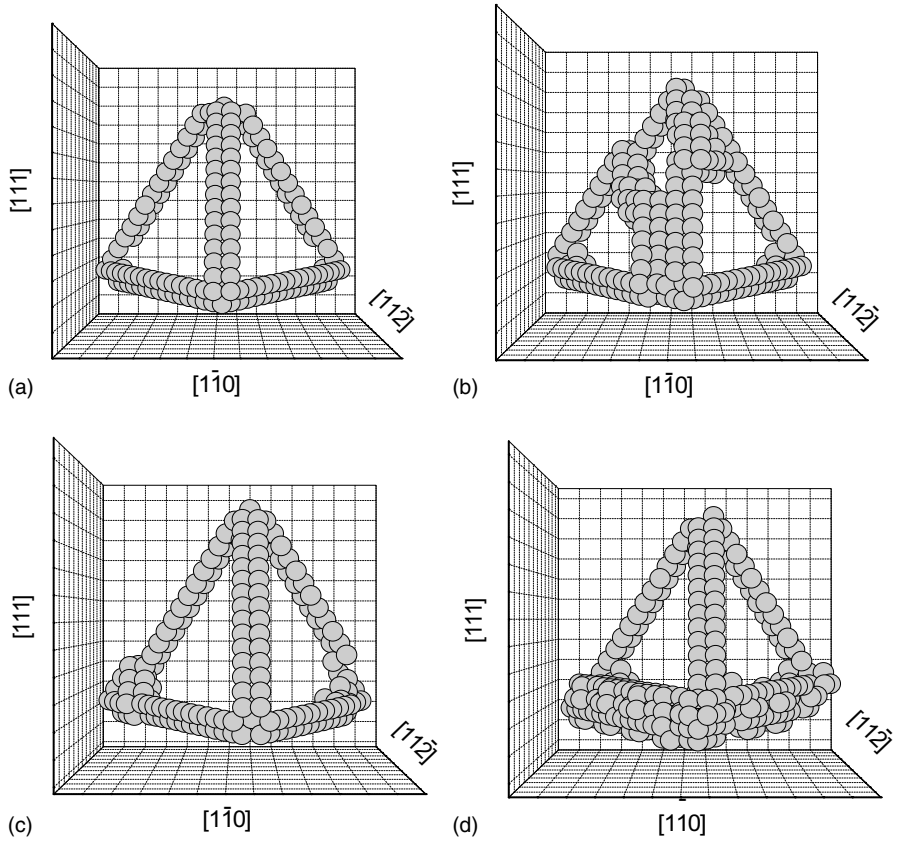

Fig. 4. Configuration of 4.1 nm SFT (a) before and (b–d) after interaction with the dislocation gliding at different h: (b) $h = 0.96$ nm, (c) $h = 0.48$ nm and (c) $h = 0$.

by many dislocations formed from the same source gliding in the same and close slip planes [12]. That means the same obstacle, i.e. SFT, can be cut many times by dislocations in the same and/or close slip planes. We have investigated such cases and found that the result again depends on h. For large h, e.g. when slip plane is close to the vertex, SFT cannot be damaged and it restores perfect configuration after every dislocation passes through. In the case of small h, when ledges can be formed, the SFT can be broken into pieces separated proportionally of the number of dislocations passed. An example of configuration of a 2.5 nm SFT, containing 45 vacancies, after multiply dislocation cut is presented in Fig. 5. The first dislocation, Fig. 5(1) (the number of the configuration in Fig. 5 indicates how many dislocations passed through), created a pair of ledges described above whereas next dislocations shift the upper part of the SFT towards the Burgers vector direction. In the case described the dislocations move from the right to the left. The forth dislocation separates completely a small perfect SFT containing 21 vacancies and a 24 vacancies cluster with two parallel stacking faults, one of

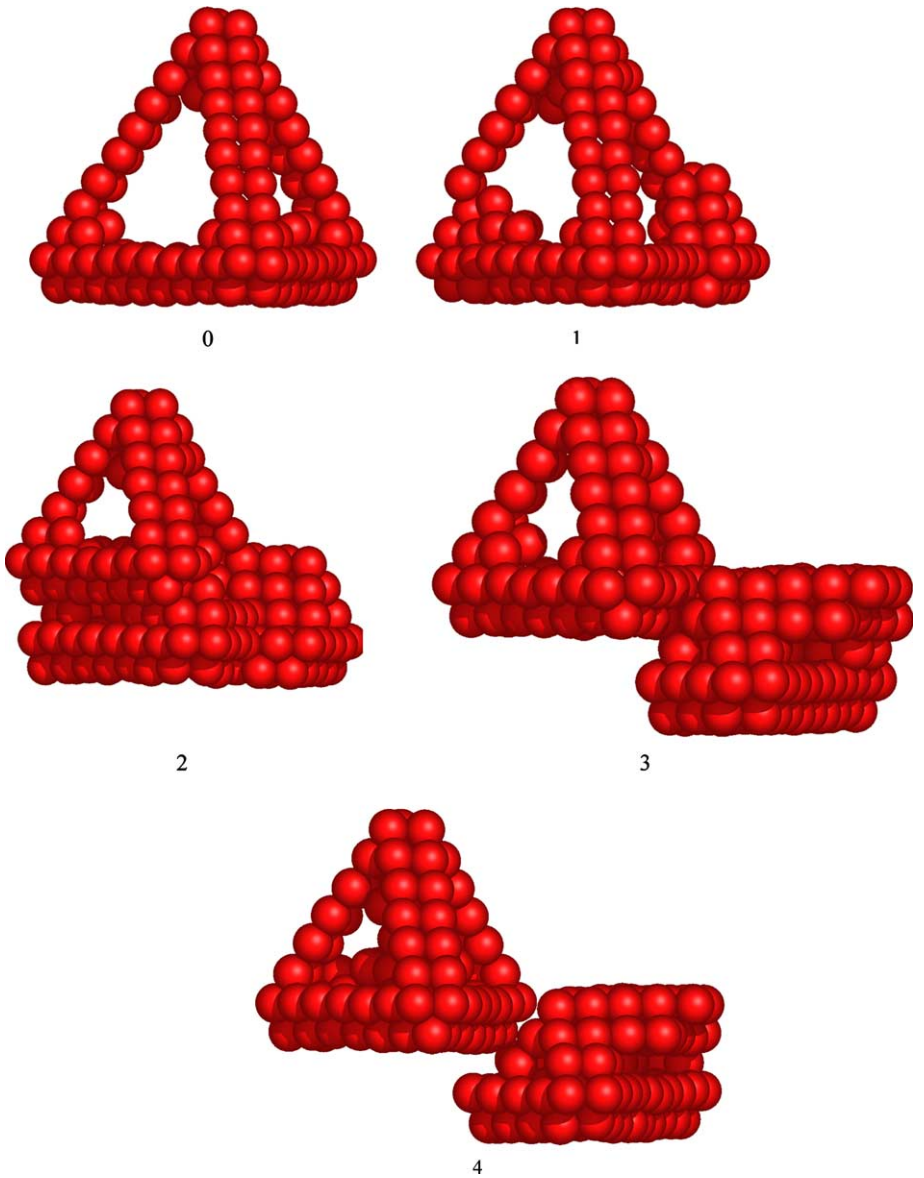

Fig. 5. Configuration of 2.5 nm (45 vacancies) SFT (0) before and (1–4) after interactions with the dislocation gliding through its centre. The number near each configuration indicates how many time the dislocation passed through.

which is the former SFT base and the other one is created due to interaction. We did not identify the structure of the lower cluster but it is definitely that of low binding energy and, therefore, should be either dissociated or transformed, e.g. to Frank loop, depending on time and temperature. It is interesting to note that the upper part of the SFT is undamaged and this is consistent with experimental TEM observations during in situ deformation of quenched and annealed gold [5].

3. Conclusions

Interaction between a moving edge dislocation and stacking fault tetrahedra of size from 2.5 to 4.1 nm has been studied at atomic scale by molecular dynamics and statics techniques. The critical resolved shear stress depends strongly on the geometry of the interaction and the crystal temperature: CRSS decreases at higher temperature and larger distance, h, between the dislocation glide plane and the SFT base parallel to it. Depending on h SFT can be damaged or not. The damage includes creation of two ledges of the opposite signs on SFT's faces cut by the moving dislocation. Creation of ledges decreases SFTs stability and can serve as initiation of their dissolution. The latter observed commonly in in situ deformation TEM experiments [4,5] however more detailed study is necessary for full understanding of the atomic-scale mechanisms involved. Note, that in general the damage of SFTs depends on its size and structure. Thus a significant damage of 2 nm SFT by an edge dislocation was reported in [8] and a complete absorption of two overlapping non-perfect SFT was observed in [13]. At least two other feature of SFT–dislocation interaction (1) when the SFT changes its TEM contrast when dislocation approaches and restores it when dislocation comes through and (2) when the lower (relatively to the slip plane) part of an SFT disappears due to interaction whereas the upper one remains undamaged, were experimentally observed in gold [5] and are consistent with MD studies reported here.

The SFTs studied here are related to irradiation conditions, when maximum of size distribution is about 2.5 nm, rather than to in situ experiments, when the size is of the order 20–50 nm. Such a considerable difference can lead to a difference in the mechanism of dislocation–SFT interaction. More atomic-scale studies are necessary to clarify effects involved in plastic instability and creation of cleared channels in irradiation and non-irradiation conditions. Particularly, those for (a) screw dislocations, (b) SFTs of larger size, when dislocation–SFT reaction may become closer to a dislocation-(stair rod) dislocation reaction, (c) lower strain rates, when the time of the interaction became long enough to involve diffusion mechanisms and (d) thin film conditions (as in in situ TEM experiments where the specimen thickness is about 100 nm), when the slow moving dislocation may serve as a channel for defect (vacancy) transport to close strong sinks, e.g. surface.

Acknowledgements

The authors thank Professor D.J. Bacon and Drs S. Zinkle, S.I. Golubov, B.N. Singh, D. Rodney and B. Wirth for numerous stimulating discussions of experimental and simulation results.

References

[1] B.N. Singh, S.J. Zinkle, J. Nucl. Mater. 206 (1993) 287.
[2] J. Silcox, P.B. Hirsch, Philos. Mag. 4 (1959) 72.
[3] M. Kiritani, Mater. Sci. Eng. A 350 (2003) 1.
[4] J.S. Robach, I.M. Robertson, B.D. Wirth, A. Arsenlis, Philos. Mag. 83 (2003) 955.
[5] Y. Matsukawa, S.J. Zinkle, these Proceedings.
[6] M. Hiratani, H.M. Zbib, B.D. Wirth, Philos. Mag. A 82 (2002) 2709.
[7] B.D. Wirth, V.V. Bulatov, T. Diaz de la Rubia, J. Eng. Mater. Technol. 124 (2002) 329.
[8] Yu.N. Osetsky, D.J. Bacon, B.N. Singh, B. Wirth, J. Nucl. Mater. 307–311 (2002) 852.
[9] Yu.N. Osetsky, D.J. Bacon, in: Mesoscopic Dynamics in Fracture Process and Strength of Materials, IUTAM Symposium Proceedings, July 2003, Osaka, Kluwer Academic, in press.
[10] Yu.N. Osetsky, D.J. Bacon, Modell. Simul. Mater. Sci. Eng. 11 (2002) 427.
[11] G.J. Ackland, G. Tichy, V. Vitek, M.W. Finnis, Philos. Mag. A 56 (1987) 735.
[12] M. Victoria, N. Baluc, C. Bailat, Y. Dai, M.I. Luppo, R. Schaublin, B.N. Singh, J. Nucl. Mater. 276 (2000) 114.
[13] B.D. Wirth, V.V. Bulatov, T. Diaz de la Rubia, J. Eng. Mater. Technol. 124 (2002) 329.